Conformable large-area position-sensitive photodetectors based on luminescence-collecting silicone waveguides

Petr Bartu,[1,a] Robert Koeppe,[1,2] Nikita Arnold,[1] Anton Neulinger,[1] Lisa Fallon,[3] and Siegfried Bauer[1]
[1]*Department for Soft Matter Physics (SoMaP), JKU Linz, Altenberger Strasse 69, 4040 Linz, Austria*
[2]*isiQiri interface technologies GmbH i.G., c/o tech2b, Hafenstr. 47-51, 4020 Linz, Austria*
[3]*Dublin Institute for Advanced Studies (DIAS), 31 Fitzwilliam Place, Dublin 2, Ireland*

(Received 13 January 2010; accepted 25 April 2010; published online 16 June 2010)

Position sensitive detection schemes based on the lateral photoeffect rely on inorganic semiconductors. Such position sensitive devices (PSDs) are reliable and robust, but preparation with large active areas is expensive and use on curved substrates is impossible. Here we present a novel route for the fabrication of conformable PSDs which allows easy preparation on large areas, and use on curved surfaces. Our device is based on stretchable silicone waveguides with embedded fluorescent dyes, used in conjunction with small silicon photodiodes. Impinging laser light (e.g., from a laser pointer) is absorbed by the dye in the PSD and re-emitted as fluorescence light at a larger wavelength. Due to the isotropic emission from the fluorescent dye molecules, most of the re-emitted light is coupled into the planar silicone waveguide and directed to the edges of the device. Here the light signals are detected via embedded small silicon photodiodes arranged in a regular pattern. Using a mathematical algorithm derived by extensive using of models from global positioning system (GPS) systems and human activity monitoring, the position of light spots is easily calculated. Additionally, the device shows high durability against mechanical stress, when clamped in an uniaxial stretcher and mechanically loaded up to 15% strain. The ease of fabrication, conformability, and durability of the device suggests its use as interface devices and as sensor skin for future robots. © *2010 American Institute of Physics*. [doi:10.1063/1.3431394]

I. INTRODUCTION

Position sensitive devices (PSDs) are currently employed in guidance systems, machine tools, and optical alignment systems.[1] Large area applications may emerge in artificial skin for robots and for surrounding sensitive machinery, as well as for interactive human machine interfaces in computers—fields in which materials are needed that have high mechanical stability and conformability combined with easy fabrication processes. In contrast to energy-elastic crystalline solids, such as silicon traditionally used in common PSDs, entropy-elastic elastomeric silicones like polydimethylsiloxane (PDMS) seem ideally suited as they fulfill all the aforementioned requirements for large area PSD applications. Stretchable elastomers are at the heart of the fast-growing research field of "conformable electronics."[2–5] The high optical transparency makes elastomers also an ideal solution for conformable optical waveguides. Thus, such waveguides can be used to illustrate concepts in "stretchable photonics," where mechanical stretching may be employed for phase matching, light modulation or, as in this contribution, for position sensing on areas of variable size.

Research on PSDs dates back to the discovery of the lateral photoeffect by Schottky.[6] After further investigations by Wallmark, several types of position-sensitive photodetectors have been developed.[7] The most common PSDs based on the lateral photoeffect are fabricated using inorganic semiconductors and show high reliability and performance.[1,8] However, the cost of silicon technology scales strongly with the active area of the device, making large-area photosensors uncommon. Furthermore, fabrication on flexible, curved, or conformable substrates is difficult due to the energy elasticity of silicon. PSD devices based on organic semiconductors are an interesting alternative, as described for example in Refs. 9 and 10. Unfortunately, this technology is not yet mature. Especially the long-time stability and reliability still remain to be proven. Additionally, conformable large area PSDs are difficult to achieve with such concepts.

In the following, we show that a stretchable planar optical waveguide made from PDMS with embedded fluorescent dyes [Fig. 1(a)] used in combination with silicon photodiodes arranged in a regular two-dimensional (2D) lattice [Fig. 1(b)] satisfies all requirements for a functional large-area PSD, which can be simply adapted to different sizes by stretching. By exploiting the high stretchability of the elastomer, the PSD can serve as a "universal detection tool," allowing the detector to cover nonplanar surfaces of different shapes and sizes.

II. EXPERIMENTAL

A. Device fabrication

For the fabrication of our device we used the organic laser dye Pyrromethene 597 (obtained from Radiant Dyes Laser Accessories) as the fluorescent agent.[11] This dye can be dissolved in the nonpolar PDMS precursor and shows a

[a]Electronic mail: petr.bartu@hotmail.com.

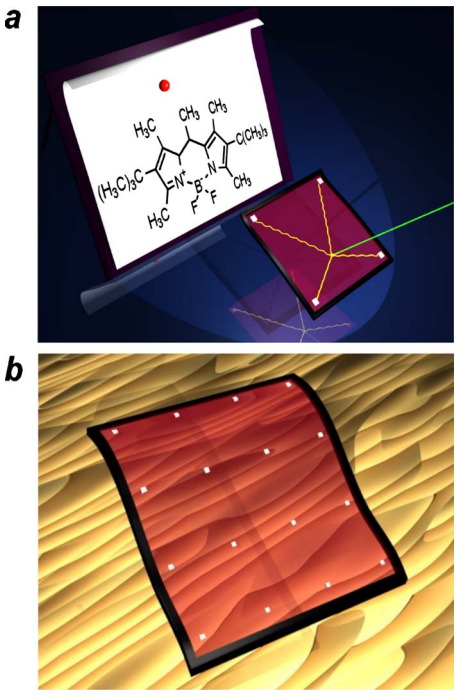

FIG. 1. (Color online) (a) Schematic drawing of the PSD fabricated from PDMS and the fluorescent dye pyrromethene 597. The laser light is absorbed by the dyes and re-emitted mostly into the planar waveguiding modes of the PDMS waveguide, where it is transported to the photodiodes in the corners of the device. The chemical structure of the dye used is shown in the background. (b) Extension to light detection on considerably larger areas using photodetectors arranged in a regular pattern.

strong fluorescence in the polymerized PDMS. 10 mg of the dye were mixed in 1 ml of ethanol. 1 μl of the solution was then added to 1 ml of the PDMS-base (Sylgard® 184 from Dow Corning) and mixed well for 24 h using a magnetic stirrer. For the fabrication of a 2D PSD, a double-sided tape was affixed to a plane glass plate to form two areas with sizes of 10×10 cm^2 and 3×3 cm^2, respectively. After mixing, the Sylgard® 184 curing agent was added to the solution (ratio base:hardener=20:1) and stirred by hand for at least 5 min. Then the mixture was filled into the mold, forming a 1.5 mm thick layer for 10×10 cm^2 samples and a 0.5 mm thick layer for 3×3 cm^2 samples. Air bubbles, which can arise during mixing, were removed by piercing with a thin needle. The curing of the PDMS was always carried out in a preheated oven at 70 °C for 1 h. After the first curing step and the subsequent cooling, four photodiodes (Osram BPW34) were placed on the 0.5 mm thick layer and the whole area was covered with an additional 0.5 mm of the PDMS-dye mixture and hardened again. Afterwards, the photodiodes were cut out and attached near the corners of the 10×10 cm^2 layer at a distance of 2 cm from the edges, marking a square with an area of 6×6 cm^2 and connected to the wires leading out of the edges. The whole device was then covered with PDMS-dye mixture up to an overall thickness of 2.5 mm and finally cured under the same conditions as described above. Due to the additional layer beneath the photodiodes, the connection wires can be sealed inside the PSD, thus fixing the photodiodes and avoiding a release from the PDMS under mechanical load. Additionally, a one-dimensional PSD stripe with 30 cm length, 2 cm width, and 2.5 mm thickness was fabricated as above, with just one embedded silicon photodiode positioned at a distance of 5 mm from the edge.

The double-sided tape was then peeled away, shifted by about 5 mm and affixed to the glass plate again. The gap was filled with a PDMS-carbon black mixture (weight ratio PDMS:carbon black powder=100:1) and cured as above. During the measurements, the PDMS-carbon black frame avoids back reflections of light from the edges.[21]

The PSDs were then peeled off the glass plate, placed on a sheet of black paper to prevent backscattering of the transmitted light and finally fixed to a computer controlled x-y-positioning stage that moves under the laser. Due to the rough surface, the contact area between the PSD and the underlying paper is very small. Thus, the light propagation in the planar waveguide is not disturbed, so that the condition (1) described in part III is fulfilled. The difference between a freestanding sample and a PSD placed on a black paper support is presented in Sec. V in detail.

B. Measurement setup

For the optical measurements we used a 10 mW, 532 nm green laser diode, which illuminates the PSD through an OD1 filter with an intensity of 0.8 mW. The light was mechanically chopped at 350 Hz. The current signals were first collected via a computer-controlled relay-switch (Quancom USBREL8A), then converted to voltages using a current-to-voltage converter (Femto DLPCA 200, gain factor 10^3), and finally measured with a lock-in amplifier (EG&G 7265). For the step-wise procedure scan we used an x-y-translation stage (Linos x.act XY-stage) with high accuracy (<0.1 mm).

III. LIGHT PROPAGATION IN THE PSD

In the proposed large area PSD shown in Figs. 1(a) and 1(b), incident light (e.g., from a commercially available weak laser pointer used for presentations) is absorbed by the dye in the PSD and re-emitted as fluorescence at higher wavelengths due to the Stokes shift. The device bears resemblance to luminescent concentrators originally developed for solar cells.[12–14] Assuming a random distribution of the transition dipole moment of the dye molecules, the emission is isotropic and most of the light is coupled into planar waveguide modes of the PDMS sheet. The radiative loss L depends on the refractive indices of the waveguide and the ambient medium, and is given by

$$L = 1 - \frac{(n^2-1)^{1/2}}{n}, \tag{1}$$

where n is the refractive index of the elastomer.[13,15] For PDMS with an $n=1.4$, 70% of the emitted light is coupled into planar waveguide modes.

Outcoupling from the PDMS waveguide modes occurs at the edges or at defects on the surface of the elastomer sheet. By embedding small silicon photodetectors in the sheet in a regular pattern [Fig. 1(b)], artificial defects are created and the light is locally coupled into the detectors,

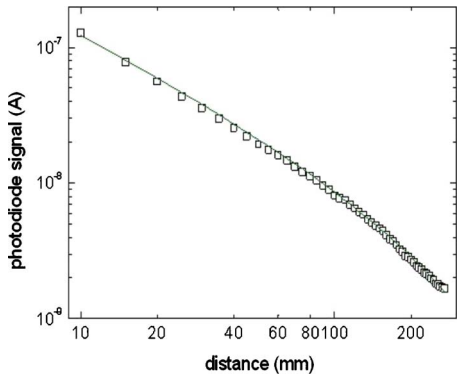

FIG. 2. (Color online) Measured photodiode signal versus distance to the photodiode (squares), fitted by the expression $I_i = Ae^{-\alpha l_i}/l_i$ (solid curve).

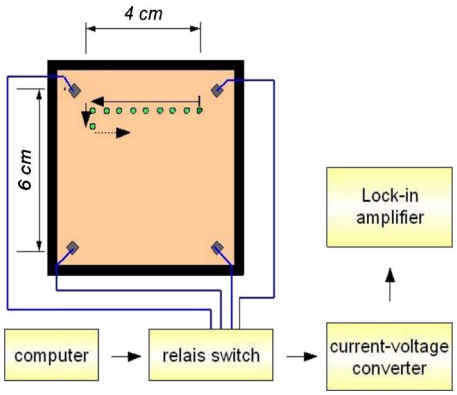

FIG. 3. (Color online) Schematic drawing of the measurement sequence following a regular serpentine pattern indicated by dots and arrows. The current amplitudes of the photodiodes are collected via a computer-controlled relay-switch, converted to voltage signals, and measured by a lock-in amplifier.

creating an electrical signal. This is in contrast to luminescent concentrators for solar cells, as described in Ref. 16, where the solar cells are mounted only on the side of the waveguide to harvest as much light as possible. A similar device consisting of a thin and flexible polycarbonate foil doped with luminescent dyes has been presented recently in Ref. 17, where a large number of silicone photodiodes can be used to detect an impinged laser light in high speed.

To investigate the signal attenuation versus the distance to the photodiode in a one-dimensional case, we fabricated a one-dimensional stripe detector as described in the experimental section. The photodiode was connected to the readout circuit, and the amplitudes of the photodiode current were collected. After each measuring step, the sample was shifted by 5 mm. As can be seen in the log-log-diagram in Fig. 2, the dependence of the observed current signals on the distance between light spot and photodiode can be fitted very well with expression (2):

$$I_i = A\frac{e^{-\alpha l_i}}{l_i}, \tag{2}$$

where A is the amplitude, α is the extinction coefficient, and l_i are the distances between the light source and the detectors. The decrease in the current signal due to absorption, scattering and outcoupling losses is given by $\exp(-\alpha l_i)$, whereas the $1/l_i$ dependence describes energy conservation as the light spreads out in the waveguide. In our case of a linear waveguide with suppressed back reflection of light from the edges, the device behaves like an infinitely sized 2D waveguide. The curve fit in Eq. (2) results in a weak extinction coefficient of $\alpha = 4.1 \times 10^{-3}$ mm^{-1} and an amplitude of 1.28×10^{-6} A mm.

IV. 2D POSITION DETECTION

Motivated by the results from the previous experiment, we investigated the light propagation in the 2D PSD. The area between the photodiodes was scanned stepwise in a regular serpentine pattern, as illustrated in Fig. 3. For each step, the current amplitudes of all photodiodes were collected as described in the experimental section. Starting, turning and ending points were positioned at a distance of 1 cm from the photodiodes, resulting in a scanning area of 4×4 cm^2 with a step size of 5 mm in x- and y-direction. Therefore, silicon photodiodes with a total active area of 28 mm^2 can be used to measure signals over an area of 16 cm^2, increasing the active area of the photodiodes by a factor of 57.

In Fig. 4, the resulting three-dimensional (3D) landscapes of the measured signals versus the x-y-positions are presented. As the coupling of light into the photodiodes is sensitive to the surroundings and exact orientation of the diodes, the amplitude A_i has to be calibrated separately for each detector. After calibration, the exact x-y position of the laser spot can be determined unambiguously from the measured current signals and plots similar to Fig. 4. For the general development, it is convenient to compensate for light-coupling differences by introducing the common amplitude $\bar{A}$. In all subsequent formulas we imply renormalized signals $\bar{I}_i \equiv I_i \bar{A}/A_i$, whereas for the amplitude A we imply $\bar{A}$, which is the same for all detectors and which can be chosen arbitrarily. Detailed calculations and a schematic explanation of the notations are given in Ref. 21.

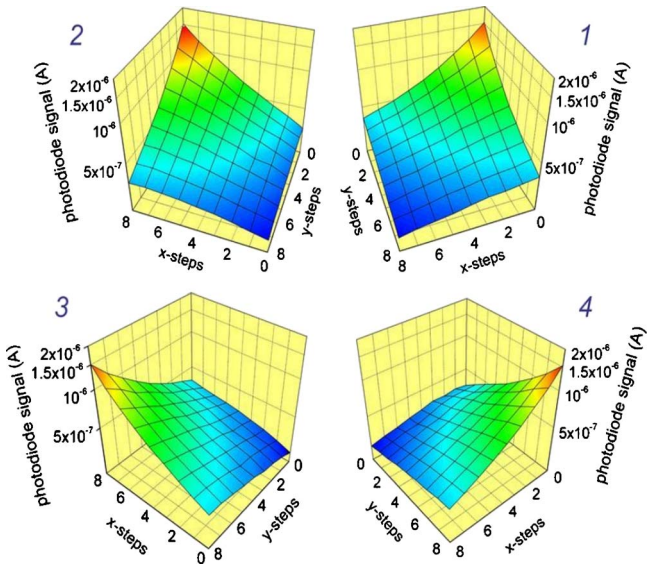

FIG. 4. (Color online) 3D plots of the measured signals I_i, with the x- and y-planes representing the rows and columns of the measuring steps, respectively. The numbers indicate the respective photodetector.

To find the exact coordinates of the light source, we first determine the distances l_i from Eq. (2). This can be done using the Lambert W-function (the inverse of xe^x),[18] resulting in

$$l_i = \frac{1}{\alpha} W\left(\frac{A\alpha}{I_i}\right). \tag{3}$$

If the distances from the light source to all detectors are known, determination of its position resembles the lateration problem. Such problems are studied extensively in connection with global positioning system (GPS) technology and human activity monitoring.[19,20] Particular to our case are the 2D instead of the 3D geometry, and the determination of distance from signal attenuation instead of delay times. Simple expressions for the position calculation can be found for small extinction coefficients $\alpha l_i \ll 1$. In this case, the Taylor expansion of Eq. (2) results in the following expression for the amplitude

$$B \equiv A\alpha \approx \frac{1}{2} \times \frac{I_1^{-2} - I_2^{-2} + I_3^{-2} - I_4^{-2}}{I_1^{-3} - I_2^{-3} + I_3^{-3} - I_4^{-3}} \tag{4}$$

Using Eq. (4) and given small extinction, one obtains for the light source coordinates:

$$x_0 = \frac{-l_1^2 + l_2^2 + l_3^2 - l_4^2}{8a} \approx \frac{-I_1^{-2} + I_2^{-2} + I_3^{-2} - I_4^{-2}}{8a} \underbrace{B^2\alpha^{-2}}_{A^2}, \tag{5}$$

$$y_0 = \frac{-l_1^2 - l_2^2 + l_3^2 + l_4^2}{8a} \approx \frac{-I_1^{-2} - I_2^{-2} + I_3^{-2} + I_4^{-2}}{8a} \underbrace{B^2\alpha^{-2}}_{A^2}. \tag{6}$$

Here, $2a$ represents the distance between the two neighboring photodiodes and A is the signal amplitude, which enters into Eqs. (2)–(4). Expressions (5) and (6) can be obtained either as an exact solution for a set of ideal noiseless data or from the linearized error minimization for a redundant set of measured data.

To decrease the influence of experimental errors (mainly related to direction-sensitive coupling of light into the photodiodes), which is especially important in the denominator of the right hand side in Eq. (4), A, or more accurately $B \equiv A\alpha$, is first calculated for all measured points using Eq. (4) and set to its average value. This common value, which depends only on the measured signals, is used to determine the x- and y-positions from Eqs. (5) and (6). The extinction coefficient α is a common scaling factor that should minimize the discrepancy between the observed and calculated positions. This results in an average deviation of 1.36 mm and $\alpha = 2.85 \times 10^{-3}$ mm^{-1}. Final calculated positions can be seen in Fig. 5. After a single calibration scan yielding the renormalization factors of the signals and the common scaling factor B, the position can be calculated accurately from the measured signals using the relatively simple expressions in Eqs. (5) and (6). The equations can be implemented in a simple algorithm allowing fast determination of the exact position with rather basic electronic readout systems.

The mean deviation of the calculated positions is smaller than the size of the photodiodes (active area 2.65 $\times 2.65$ mm^2) and is of the same order as the radius (2 mm) of the laser spot. Small variations in the PDMS sheet thickness and the anisotropic coupling of the light into the photodiodes lead to systematic errors in the position calculation. In

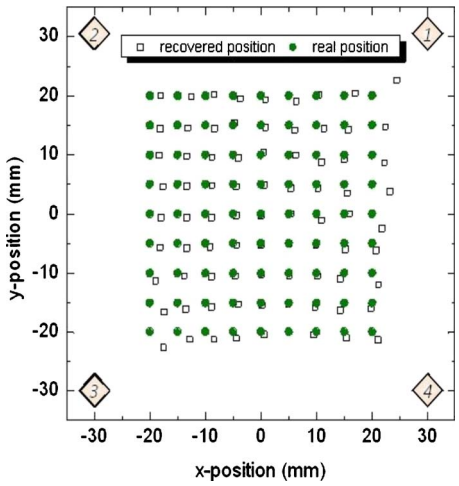

FIG. 5. (Color online) Calculation of the positions in the x-y-plane based on the observed signals. Numbered squares denote the respective photodetectors.

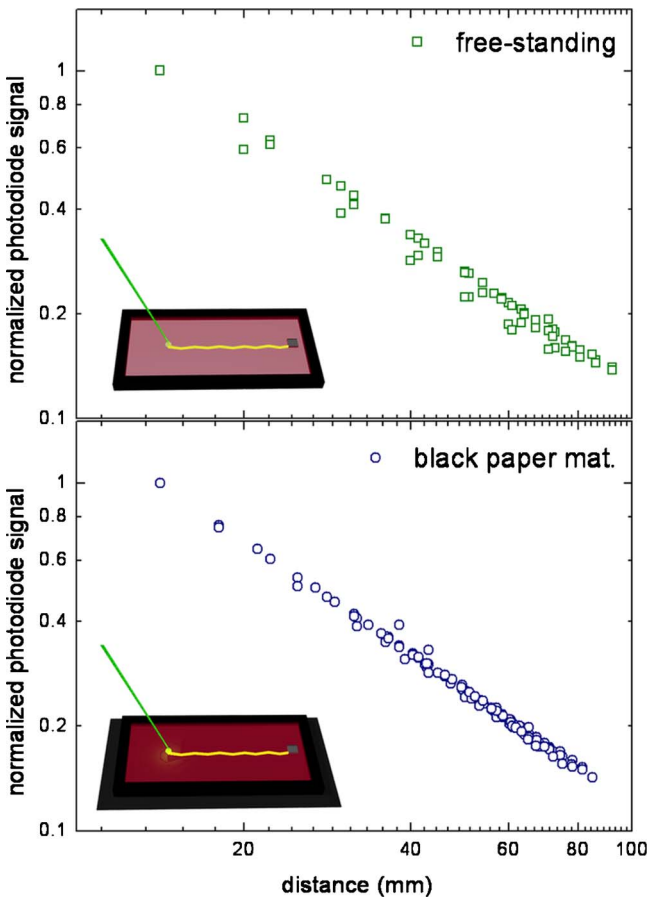

FIG. 6. (Color online) A comparison of the light attenuation between a free-standing PSD and a PSD placed on a sheet of black paper. The measurements show no significant differences in the light propagation under these largely different conditions. The extinction coefficient α is 2.05×10^{-3} mm^{-1} for the free-standing PSD and 2.25×10^{-3} mm^{-1} for the PSD placed on the black paper support, respectively.

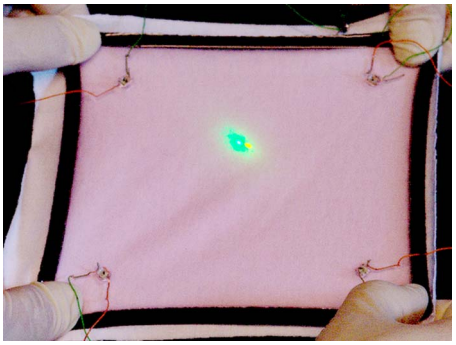

FIG. 7. (Color online) The fabricated device is flexible and can assume different, in particular also curved, shapes. Operation is possible with light impinging directly on the PSD (as shown here) or through the translucent white board or screen. In this case the device can be used in combination with a video projector, where video games as well as interactive presentations can be projected onto the white screen.

cases where high accuracy is more important than readout speed and ease of fabrication, these can be corrected by a point-for-point calibration of the device. However, in general, Eqs. (5) and (6) or their generalizations for arbitrary extinction (see Ref. 21) serve as a basis for a universal algorithm to extract absolute position values from similar devices without the need of this calibration step.

V. WAVEGUIDE EXTINCTION WITH AND WITHOUT SUPPORT

In order to determine effects of a paper support on the light extinction, a free-standing stripe detector has been compared with a detector placed on a black paper, simulating extreme conditions of use. As shown in Fig. 6, there is only a weak change in the normalized photodiode signals for the two detector configurations, showing that the PSDs can be used either free-standing or placed in front or behind a translucent screen.

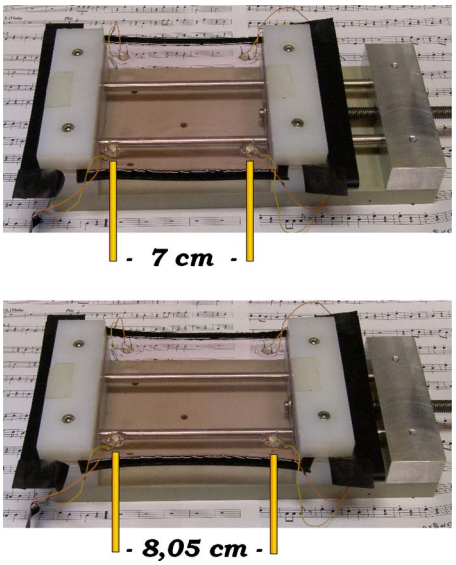

FIG. 8. (Color online) PSD clamped into a uniaxial stretcher; (a) 0% stretch and (b) 15% stretch ratio.

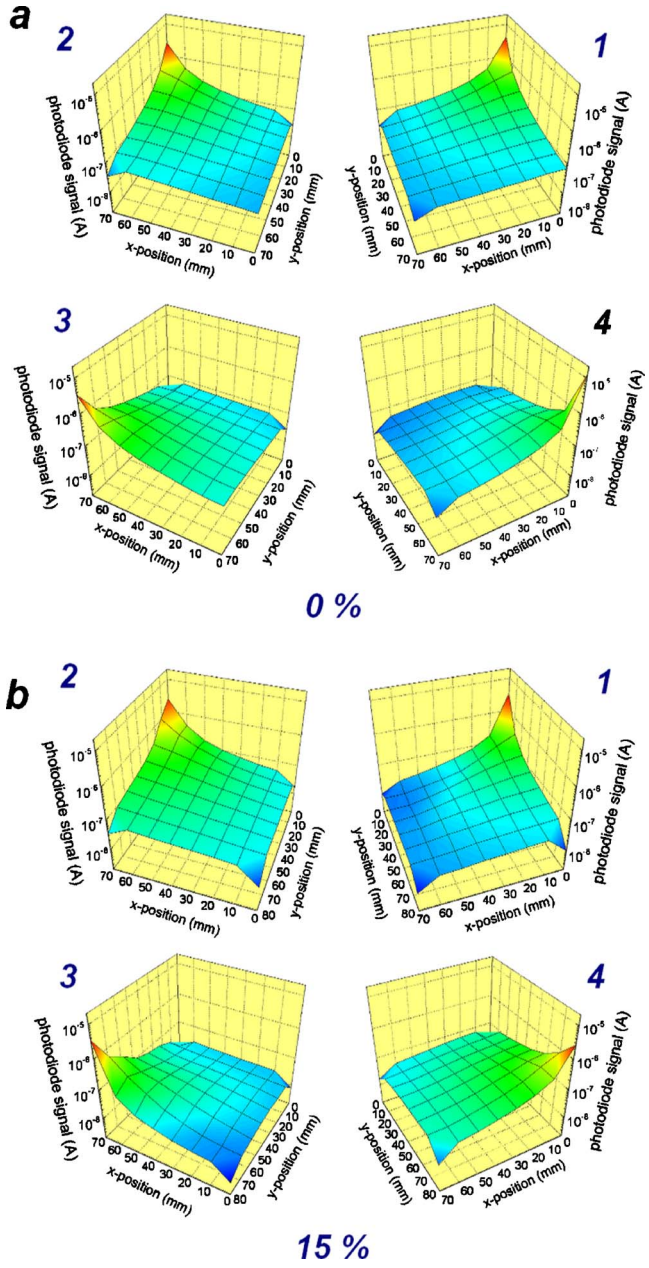

FIG. 9. (Color online) Influence of stretching. 3D plots of the observed signal amplitudes; (a) unstretched, (b) uniaxially stretched by 15% in the y-direction. The x- and *y*-axis indicate the distance between the measured photodiode signal and the starting point (photodiode 1), the numbers indicate the respective photodetectors.

The measurements with the free-standing and supported PSD demonstrates the versatility of the concept for large area position sensing. In Fig. 7, a possible application is shown, where a stretchable whited board placed in front of the PSD can be used as a projection screen.

In this case, the device can be used in combination with a video projector, giving the user the opportunity of performing video games as well as presentations projected onto the white screen.

VI. MECHANICAL STRETCHING

To test the mechanical strength of the device, a second 2D PSD was prepared with the photodiodes placed in the

corners of a 7×7 cm^2 square. The sample was clamped into a custom-built manually controlled uniaxial stretcher fixed to the x-y-positioning stage. The sample was then stretched uniaxially in the y-direction by 0% to 15% in 5%-steps and measured under the same conditions as in the previous experiment. Figure 8 show photographs of the fabricated PSD clamped into a uniaxial stretcher unit, (a) depicts the unstretched and (b) the 15% stretched state, respectively.

To keep better track of the measured area during the stretching procedure, the starting, turning and ending points were positioned directly on the embedded photodiodes. Whereas the step size of 10 mm in the x-direction was the same for all stretching conditions, the step sizes in the y-direction varied depending on the applied strain and the resulting distance between the photodiodes (from 10 mm steps for 0% to 11.5 mm steps for 15% strain).

The 3D plots of signals at each photodiode in both the unstretched and the 15%-stretched state are presented in Fig. 9 and confirm good stability under mechanical load. Lower amplitudes are observed in the corners because the laser spot partly covers the backside of the embedded photodiodes, thus decreasing the amount of light coupled into the PSD. Due to the deformation of the scanned area, a calculation of the light spot position requires extension of the model to anisotropic extinction. This will be the topic of future work.

VII. SUMMARY

In conclusion, a flexible, large-area position-sensitive device for the detection of localized light spots has been fabricated for illustrating the concept of "stretchable photonics." A mathematical model developed for precise position calculation yields accuracies comparable to the laser spot size. The device can withstand a strain of stretching up to 15% while retaining its position-sensing capabilities. Thus, this kind of sensor can be used in a wide range of applications in which both high flexibility and conformability are required.

ACKNOWLEDGMENTS

The authors would like to thank Markus Krause and Gerda Buchberger for suggestions and assistance. This work was partially supported by the Austrian Science Fund (FWF) within the National Research Network on Functional Organic Films.

[1] J. Henry and J. Livingstone, Adv. Mater. **13**, 1022 (2001).
[2] T. Someya, T. Sekitani, S. Iba, Y. Kato, H. Kawaguchi, and T. Sakurai, Proc. Natl. Acad. Sci. U.S.A., **101**, 9966 (2004).
[3] S. P. Lacour, J. Jones, S. Wagner, T. Li, and Z. Suo, Proc. IEEE **93**, 1459 (2005).
[4] D.-H. Kim, J.-H. Ahn, W. M. Choi, H.-S. Kim, T.-H. Kim, J. Song, Y. Y. Huang, Z. Liu, C. Lu, and J. A. Rogers, Science **320**, 507 (2008).
[5] 2009 Symposium PP: Materials and devices for flexible and stretchable electronics. Documented in MRS spring meeting, San Francisco, organized by S. P. Lacour, S. Bauer, T. Li, T. Someya (2009).
[6] W. Schottky, Phys. Z. **31**, 913 (1930).
[7] J. T. Wallmark, Proc. IRE **45**, 474 (1957).
[8] E. Fortunato, G. Lavareda, R. Martins, F. Soares, and L. Fernandes, Sens. Actuators, A **51**, 135 (1996).
[9] D. Kabra, T. B. Singh, and K. S. Narayan, Appl. Phys. Lett. **85**, 5073 (2004).
[10] R. Koeppe, P. Bartu, S. Bauer, and N. S. Sariciftci, Adv. Mater. **21**, 3510 (2009).
[11] J. H. Boyer, A. M. Haag, G. Sathyamoorthi, M.-L. Soong, and K. Thangaraj, Heteroat. Chem. **4**, 39 (1993).
[12] J. S. Batchelder, A. H. Zewail, and T. Cole, Appl. Opt. **18**, 3090 (1979).
[13] A. Goetzberger and W. Greubel, Appl. Phys. (Berlin) **14**, 123 (1977).
[14] R. Koeppe, N. S. Sariciftci, and A. Büchtemann, Appl. Phys. Lett. **90**, 181126 (2007).
[15] G. Keil, J. Appl. Phys. **40**, 3544 (1969).
[16] I. S. Melnik and A. H. Rawicz, Appl. Opt. **36**, 9025 (1997).
[17] R. Koeppe, A. Neulinger, P. Bartu, and S. Bauer, Opt. Express **18**, 2209 (2010).
[18] R. M. Corless, G. H. Gonnet, D. E. G. Hare, D. J. Jeffrey, and D. E. Knuth, Adv. Comput. Math. **5**, 329 (1996).
[19] J. Hightower and G. Borriello, Computer **34**, 57 (2001).
[20] Y. Nishida, H. Aizawa, T. Hori, N. H. Hoffman, T. Kanade, and M. Kakikura, Proceedings of the IEEE International Conference on Intelligent Robots and Systems (IROS2003), October 27–31 2003 in Las Vegas, 1, 785–791 (2003).
[21] See supplementary material at http://dx.doi.org/10.1063/1.3431394 for a detailed description of the fabrication process presented in Fig. 11 for details of the measurement setup.